Published in final edited form as:
*Nat Protoc*. 2014 September ; 9(9): 2123–2134. doi:10.1038/nprot.2014.141.

# Preparation of Microcrystals in Lipidic Cubic Phase for Serial Femtosecond Crystallography

**Wei Liu**[1,2], **Andrii Ishchenko**[1], and **Vadim Cherezov**[1]

Wei Liu: weiliu@scripps.edu; Andrii Ishchenko: ishchenk@scripps.edu

[1]Department of Integrative Structural and Computational Biology, The Scripps Research Institute, La Jolla, CA, USA

[2]Marine Drug Research Institute, Huaihai Institute of Technology, Lianyungang 222005, China

## Abstract

We have recently established a procedure for serial femtosecond crystallography in lipidic cubic phase (LCP-SFX) for protein structure determination at X-ray free electron lasers (XFELs). LCP-SFX uses the gel-like lipidic cubic phase (LCP) as a matrix for growth and delivery of membrane protein microcrystals for crystallographic data collection. LCP is a liquid-crystalline mesophase, composed of lipids and water. It provides a membrane-mimicking environment that stabilizes membrane proteins and supports their crystallization. Here we describe detailed procedures for the preparation and characterization of microcrystals for LCP-SFX applications. The advantages of LCP-SFX over traditional crystallographic methods include the capability of collecting room temperature high-resolution data with minimal effects of radiation damage from sub-10 μm crystals of membrane and soluble proteins that are difficult to crystallize, while eliminating the need for crystal harvesting and cryo-cooling. Compared to SFX methods for microcrystals in solution using liquid injectors, LCP-SFX reduces protein consumption by 2–3 orders of magnitude for data collection at currently available XFELs. The whole procedure typically takes 3–5 days, including the time required for crystals to grow.

### Keywords

X-ray free electron laser; XFEL; microcrystal; membrane protein; CrystFEL; G protein-coupled receptor; GPCR; lipidic cubic phase; LCP; Serial Femtosecond Crystallography; SFX

### Categories

Protein analysis; Structural Biology

Correspondence should be addressed to V.C. (vcherezo@scripps.edu).

**AUTHOR CONTRIBUTIONS** W.L. and A.I. worked out the protocols and wrote initial draft, V.C. developed the concept and wrote the manuscript.

**COMPETING FINANCIAL INTERESTS** The authors declare no competing financial interests.

## INTRODUCTION

Macromolecular crystallography is the most successful technique for high-resolution protein structure determination; however, obtaining sufficiently large crystals that are capable of sustaining radiation damage during data collection at synchrotron sources often represents a serious bottleneck. In many cases, crystallization trials of difficult eukaryotic membrane and soluble proteins and their complexes yield no larger than micron-sized crystals, hampering their structural studies. Recent advancements at hard X-ray free electron lasers (XFELs) promise a breakthrough in overcoming the radiation damage problem and enabling crystallographic data collection on those microcrystals that are in general unusable at synchrotrons[1, 2]. Currently there are two hard XFEL sources in the world capable of probing matter with atomic resolution: the Linac Coherent Light Source (LCLS) in Stanford, USA and the SPring-8 Angstrom Compact free electron Laser (SACLA) in Harima, Japan. Two additional XFELs (SwissFEL in Villigen, Switzerland and European XFEL in Hamburg, Germany) are expected to start their operation in 2017.

XFELs produce extremely bright X-ray pulses of femtosecond duration that allow recording of diffraction images from single microcrystals before their destruction, thus, outrunning radiation damage[3]. Since each microcrystal is destroyed by the powerful XFEL beam, a typical data collection protocol, termed Serial Femtosecond Crystallography (SFX), requires that a continuous supply of microcrystals intersects with the beam at random orientations. Diffraction images are collected at a rapid rate, limited by the XFEL pulse repetition rate (e.g. 120 Hz at LCLS and up to 27 kHz at the future European XFEL), the detector readout speed or the sample delivery method and apparatus. After accumulation of a few hundred thousand hits, the structure factor amplitudes are determined by Monte Carlo integration[4], and subsequently used for structure solution and refinement.

### An overview of SFX methods

Crystals for SFX data collection can be supplied either by streaming them across an XFEL beam using special injectors or by depositing them on a solid support (fixed target SFX), which is then rastered by the beam.

**SFX with liquid jets—**One of the first successful injectors for producing a stream of microcrystals dispersed in a liquid solution for SFX applications, the Gas Dynamic Virtual Nozzle (GDVN), was developed in 2008[5]. The GDVN injector uses an HPLC pump to push a suspension of microcrystals through a 50–100 μm capillary, focusing the resulting stream further with a co-flowing gas to a diameter of only few micrometers at the XFEL beam interaction point. A special anti-settling device has been introduced to overcome the problem with crystal settling during the data collection[6]. While it can be credited with the majority of structures determined by SFX to date[2,7–10], the GDVN injector nonetheless has a serious disadvantage when it comes to data collection at current XFELs. The minimum flow rate produced by the GDVN injector (10 μL/min, linear speed 10 m/s) is too fast for the pulse repetition rate of LCLS (120 Hz), resulting in only one out of each tens of thousands of crystals being hit by the XFEL pulse, while the rest of the sample is wasted. Therefore, structure determination by SFX using the GDVN injector typically requires tens to hundreds

of milligrams of purified and crystallized protein, which is beyond reach in most cases. These high requirements for the quantity of crystallized sample, however, will likely decrease when newer XFELs that work at a faster pulse repetition rate become available.

A different type of liquid injector, which operates on the principle of electrospinning and delivers microcrystals at slower flow rates (0.17–3 μL/min), has been recently developed and used for SFX data collection on photosystem II and thermolysin[11,12]. At these slow flow rates, however, the electrospun stream is prone to freezing in vacuum and requires the addition of a cryoprotectant. Further, the hit rates obtained with the electrospun injector are typically lower than with the GDVN, therefore, overall, the GDVN injector still remains the most popular instrument for SFX experiments. Other new types of liquid injectors are actively being pursued, but they have yet to be tested in real experiments to demonstrate their performance.

**LCP-SFX—**Recently, we have demonstrated that microcrystals can be delivered for SFX experiments more efficiently, with minimal waste, using lipidic cubic phase (LCP) material as a carrier matrix[13].

LCP is a transparent, gel-like material, made of about equal parts of lipids and water[14]. Upon formation of LCP, lipids self-assemble in a continuous lipid bilayer, mimicking the environment of biological membranes, while water segregates into two continuous interpenetrating channels sprawling through the mesophase. Along with a variety of different applications, LCP can be used to stabilize membrane proteins for biochemical or biophysical studies, and to crystallize them from a membrane-like environment[15]. First introduced about 18 years ago, the LCP crystallization method[16] had a relatively slow start; it was not readily embraced by many crystallography groups mostly due to the difficulties associated with the handling of such viscous and sticky material. Now, after over a decade of technology developments, the use of LCP in the crystallization of challenging proteins has been gaining momentum[15]. To date, this method has contributed over 50 unique membrane protein structures from different families, including receptors, enzymes, transporters and ion channels.

The gel-like consistency of LCP, which is often considered a disadvantage of this material, turned out to be instrumental in its utility for overcoming the problem with high protein consumption required for structure determination by SFX. A special LCP microextrusion injector was designed[13] that allowed the streaming of LCP with embedded microcrystals at very slow flow rates (0.001 – 0.3 μL/min), which made it possible to fine-tune the flow rate of crystals against the XFEL pulse repetition rate, so that the interval between pulses is just long enough to clear the damaged material out of the beam path and always expose fresh crystals to the new XFEL pulse. An LCP-SFX method, therefore, was established and successfully used at LCLS (Figure 1) to collect data on several membrane and soluble protein samples. Room temperature structures of two G protein-coupled receptors (GPCRs), the human serotonin 2B (5-$HT_{2B}$) receptor bound to ergotamine[17] and the human smoothened receptor bound to cyclopamine[13], have been published; several other structures are under processing. The LCP-SFX method enables high-resolution structure determination from micron-sized (1 – 10 μm) crystals at room temperature with minimal radiation damage.

The method eliminates the extensive and tedious crystal optimization process that is otherwise required to obtain sufficiently large crystals for traditional crystallography at synchrotron sources, and simplifies crystal handling by removing the crystal harvesting and freezing steps. Here we describe in detail the protocols of sample preparation for LCP-SFX.

**Fixed target SFX—**An alternative method for delivering microcrystals for SFX data collection is to deposit them on a solid support, and then raster it with the XFEL beam. This method may further reduce sample consumption for structure determination, but it requires special considerations, such as the choice of the material for the support, which should be sufficiently rigid but mostly transparent for X-rays; the design of the sample cell, which should keep microcrystals hydrated and also prevent them from being preferentially oriented along the substrate; the rastering pattern, which should allow for fast data acquisition that matches the XFEL pulse repetition rate and ensures efficient sample coverage; and others. The work on implementing serial crystallography with fixed targets both at XFELs and synchrotrons is ongoing[18–21]; however, some of the above mentioned requirements may be difficult to fully satisfy.

## EXPERIMENTAL DESIGN

### General considerations

In order to use the LCP-SFX approach, researchers must first apply for and be awarded beamtime on one of the available hard XFEL sources. Apart from securing access to an XFEL source, LCP-SFX data collection requires the use of an LCP injector[13] and of special protocols for sample preparation, described below. The primary goal of these protocols is to obtain ~50 μL of LCP that is uniformly filled with microcrystals (<10 μm in size) at a high density. This is typically achieved through a two-stage process. The first stage involves high-throughput crystallization screening in nanoliter volumes using special LCP robots in order to find suitable conditions that lead to a high rate of nucleation and the formation of a large number of microcrystals. Protocols for setting up high-throughput LCP crystallization trials and crystal detection have been published elsewhere[22–25]. These protocols are currently being routinely used in many laboratories. Once a suitable crystallization condition is found, the next stage of the process involves scaling up the crystallization volume by about 1,000 times. This scale up process is not trivial due to the gel-like texture of LCP and the slow diffusion of soluble components through it, which leads to transient concentration gradients, the extent and time-dependence of which strongly depend on the volume and shape of the LCP crystallization bolus. This article describes new optimized protocols, and other special considerations, for achieving samples with a high density of microcrystals in LCP with a total volume of ~50 μL that are suitable for collecting a complete dataset by LCP-SFX at an XFEL source. A flowchart of the process is shown in Figure 2. It begins with reconstitution of the membrane protein of interest in LCP, and then proceeds to setting up the crystallization experiments in gas-tight syringes.

Protein-laden LCP is extruded from one syringe into a precipitant solution in several other syringes as a ~400 μm (diameter) string, closely mimicking the geometry employed during initial high-throughput crystallization experiments in glass sandwich plates, but in a much larger LCP volume. The syringes are then sealed and incubated at 20 °C to allow the crystals

to grow. At this stage the samples can be transported to the beamline inside a Greenbox thermal management system (ThermoSafe Brands), equilibrated at 20 °C. After sufficient incubation time to allow microcrystals to nucleate and grow has elapsed, the precipitant solution is discarded and the LCP sample with embedded microcrystals is consolidated into one syringe. The lipid composition of the sample is then adjusted, if necessary (see section on Lipid Phase Behavior below). Finally, the crystal density and size distribution are characterized and adjusted, and the sample is transferred into an LCP injector for SFX data collection. To minimize the chance of clogging the injector nozzle, the lipid as well as protein and precipitant solutions should be pre-filtered, syringes and needles should be thoroughly cleaned, and all manipulations where sample is exposed to air should be performed inside a clean-room flow hood.

### LCP host lipid selection

Lipids that form LCP, suitable for LCP-SFX applications, are listed in Table 1. All of these lipids belong to a large class of monounsaturated monoacylglycerols (MAGs). Monoolein (9.9 MAG) has been the most successful lipid used for LCP crystallization to date[26], however, several other MAGs have proven superior to monoolein in certain cases[27,28]. Each different host lipid makes LCP with a different lipid bilayer thickness and water channel diameter, as well as responds differently to precipitant solutions, thereby affecting stability, diffusion and interaction of the reconstituted membrane proteins. In some cases, doping LCP with phospholipids or cholesterol may improve crystal growth and quality[28–30].

### Lipid phase behavior

Most MAG lipids have a very similar temperature-composition phase behavior, as schematically illustrated in Figure 3. The phase boundary locations, however, are different for each lipid (see the following publications for detailed phased diagrams of several MAGs[31–34]). The initial reconstitution of a protein into the lipid bilayer of LCP is performed at room temperature and at close to the maximal hydration capacity of LCP, which is just below the full hydration boundary (marked by an asterisk in Figure 3). For most MAGs this corresponds to the aqueous content of 40–50 % w/w (Table 1). When a membrane protein sample that has been solubilized in detergent is added to LCP and then overlaid with a precipitant solution, these phase boundaries can shift, and in some cases LCP can transform into a different mesophase[35–37]. It is therefore important to verify that the final mesophase in which microcrystals are grown is an LCP, which is indicated by a gel-like appearance and the lack of birefringence, except for the birefringence that comes from microcrystals.

When LCP, loaded with microcrystals, is extruded into vacuum, rapid evaporative cooling can induce the transition into a crystalline Lc phase (Figure 3). This is a common occurrence when monoolein is used as a host lipid, because the equilibrium LCP-to-Lc transition temperature for monoolein is 18 °C[32], only a few degrees below room temperature. The transition to Lc phase may physically damage the crystals, and, moreover, result in an excessive powder diffraction from the crystalline lipid that can oversaturate the detector. We have established that this problem can be eliminated when either 7.9 MAG or 9.7 MAG is used as a host lipid[13]. In those cases when crystal growth requires LCP made of 9.9 MAG,

the problem of lipid freezing upon extrusion in vacuum can be overcome by adding 7.9 MAG post crystal growth, as described in these protocols (Steps 22–24).

### Using LCP as a carrier medium for microcrystals of soluble proteins

The LCP-SFX method was developed originally for the structure determination of membrane proteins crystallized in LCP. The method, however, can also be applied to soluble proteins in order to dramatically reduce the amount of protein required for structure determination by SFX. It has been shown that small soluble proteins, such as lysozyme or thaumatin, can be crystallized directly in LCP[38,39]. More generally, microcrystals of a soluble protein, obtained by any crystallization method, can be mixed with an LCP host lipid (see Box 1). This method, however, works only when LCP is compatible with the precipitant solution used for crystallization. LCP that is made of monoolein as the host lipid is, in general, the most stable towards addition of various precipitants used in protein crystallization[35].

### Crystal density and hit rate

One of the most important considerations for successful data collection by LCP-SFX is a high density of crystals, which ensures a high hit rate. The hit rate depends on several parameters including the crystal size, the density of crystals, the injector nozzle diameter, and the X-ray beam size. The optimal hit rates are ~30%; lower hit rates require an increasing amount of time for data collection, while at higher hit rates the probability of multiple hits increases, making SFX data collection less efficient. While crystals obtained in a liquid solution can be easily concentrated or diluted, crystals grown in LCP can only be diluted, and not concentrated. Therefore, it is imperative to achieve the highest as possible density of crystals grown in LCP, which further could be adjusted if necessary. The two-stage protocol described here is designed to first optimize the conditions for achieving the highest crystal density using high-throughput screening with nanoliter sample volumes, and then scaling up the crystallization LCP volume while mimicking closely the conditions and geometry that was used during the high-throughput screening.

### Limitations

The most important limitation of this method is the requirement for maintaining LCP during the crystal growth. Some commonly used precipitants may transform LCP into a lamellar, hexagonal or sponge phase[35]. While lamellar and hexagonal phases, in general, do not support crystallization and therefore should be avoided, sponge phase can provide a preferred environment for growing crystals of large membrane proteins and complexes[40,41]. Sponge phase, however, behaves just like a liquid and, thus, it is not compatible with the LCP injector and this protocol. Crystals grown in sponge phase have been delivered by a GDVN injector for SFX data collection[10], but as any other samples that have used the GDVN, samples prepared in the sponge phase suffer from the problem of high crystal consumption at currently available XFELs. In certain cases it may be possible to lower the concentration of the sponge-inducing component of the precipitant solution (such as PEG400, MPD, Jeffamine M-600, etc.[40]) post crystal growth and transform the sponge phase back into LCP, however, such a procedure is not always straightforward and may affect the crystal quality.

### Other applications

Although developed specifically for data collection at XFELs, the LCP injector may find suitable application at modern synchrotron sources. It has been recently shown that the combination of high-brilliance X-ray beams with fast readout detectors can allow one to outrun the propagation of free radicals, and thus substantially increase the resistance of crystals to radiation dose at room temperature[42]. Continuous shutterless data collection at acquisition rates above 10 Hz holds promise for obtaining crystallographic data from medium sized crystals (10–50 μm) at room temperature. Thus, using an LCP injector that produces a 50–100 μm diameter stream at slow flow rates (~0.1 mm/s) may serve as a convenient way to provide a steady supply of fresh crystals for this application. Protocols described in this article are also directly applicable to the sample preparation for such serial crystallography approach at synchrotron sources.

## MATERIALS

### REAGENTS

LCP host lipid (Nu Chek Prep, Sigma, Avanti Polar Lipids) (Table 1). The host lipid would be chosen based on selected microcrystal hits from high-throughput crystallization screening (described in Refs. 22–25). See sections on “Host Lipid Selection” and “Lipid Phase Behavior” for more information.

OPTIONAL. Phospholipids, cholesterol (Avanti Polar Lipids)

Purified protein solution concentrated to 20–50 mg/mL

Precipitant solutions (based on selected microcrystal hits from high-throughput crystallization screening (described in Refs. 22–25))

**CRITICAL** Microcrystal hit conditions may include buffers, salts, polymers, volatile and nonvolatile organic solvents, additives and ligands. It is advisable to explore small concentration gradients of the main precipitant and salt if the exact condition found through the high-throughput screening is not reproducible when crystallization is scaled up in syringes.

Chloroform. **CAUTION** toxic/irritant. Wear protective gloves and safety glasses, and perform all manipulations under a fume hood. Always use glassware, stainless steel or Teflon and avoid other plastics for transferring and storing chloroform.

Methanol. **CAUTION** flammable/toxic. Wear protective gloves and safety glasses, and perform all manipulations under a fume hood.

### EQUIPMENT

Eight 100 μL Gas-tight syringes with removable needle (Hamilton, Cat. No. 81065)

Syringe coupler (Formulatrix, SKU 209526)

Removable flat-tipped needle for loading samples into LCP-injector (1 inch, point style 3, gauge 22, small hub; Hamilton, Cat. No. 7804-01)

Parafilm, cut in 2 inch × 1 inch strips

Lint free lens cleaning tissues (Fisher Scientific, Cat. No. NC9592151)

Centrifugal filter tubes, Ultrafree-MC, 0.5 mL, Durapore 5 μm (Millipore, Cat. No. UFC3 0SV 00)

Microscope slides, 1 inch × 3 inch (GoldSeal, Cat. No.3010)

Microscope cover slips, 1 inch × 1 inch (Fisher Scientific, Cat. No. 12-548C)

Two wash bottles with fine tips. One filled with milli-Q or distilled water, the other with methanol. These are used to clean the syringes, needles and coupler. Methanol is used first, then water

Zip lock bags

Powder-free gloves

Safety glasses

Pressurized air can for blow-drying syringes, needles, ferrules, and couplers

Greenbox 12 (Tegrant Corporation, Thermosafe Brands, model 12UC4) for transporting or shipping samples to the beam line

Dry block heater with a digital temperature controller (Fisher Scientific, Cat. No. 11-720-10BQ)

Centrifuge (Fisher Scientific, Cat. No. 05-413-340)

Clean Room Mini - 12 inch Portable Positive Pressure Hood with HEPA filter (Sentry Air Systems, Inc.)

20 °C incubator

Stereo zoom microscope equipped with a linear polarizer and rotating analyzer (Leica, Nikon, Olympus)

OPTIONAL. UV microscope (JAN Scientific, Formulatrix)

OPTIONAL. SONICC imager (Formulatrix)

**LCP injector—**An LCP injector is required for streaming samples produced in these protocols for LCP-SFX data collection. The original design of the injector has been described in Ref. 13; detailed drawings are available from the authors upon request.

## REAGENT SETUP

**OPTIONAL. Lipid mixing—**To supplement an LCP host lipid with any lipophilic substance, such as hydrophobic ligand, cholesterol or phospholipid, combine the required compound amounts in a glass vial, dissolve them in a minimal volume of chloroform, remove excess solvent by blowing a gentle stream of inert gas (argon or nitrogen), remove solvent traces under vacuum, flush with inert gas and store at −20 °C or below.

**LCP host lipids—**Melt and filter LCP host lipids or lipid mixtures using 5 μm pore size centrifuge filter tubes (5 min at 5,000 g), and then aliquot in small fractions (~100–200 μL), flush with an inert gas (argon or nitrogen) and store at −20 °C or below.

<TROUBLESHOOTING>

**Precipitants—**Filter precipitant solutions using spinning filter tubes (5 μm pore diameter membrane).

**CAUTION** Some of the reagents used in crystallogenesis and protein purification may be toxic, please refer to the relevant safety data sheets (SDS) and follow the instructions.

**Protein—**Centrifuge purified and concentrated protein solution at 14,000 *g* for 5 min at 4 °C to remove aggregates before mixing with lipids.

**CRITICAL** Fibers, dust, protein aggregates or other impurities may cause potential clogs in the LCP-injector, therefore all solutions and chemicals need to be filtered, all devices need to be cleaned carefully before sample preparation and loading the sample reservoir.

**CRITICAL** A consistent quality of membrane protein samples and precipitant components is important for the reproducibility of crystal formation. Protein should be used immediately after purification if possible.

## EQUIPMENT SETUP

**Needle stoppers—**Cut five needles, supplied with 100 μL gas-tight syringes, to about 5–10 mm in length and flatten their tips with pliers; to be used for plugging syringes during incubation.

**Cleaning—**All syringes, needles and couplers should be thoroughly cleaned with methanol and water, and blow-dried using compressed air. Do not touch any components that may get in contact with lipid or protein with bare hands.

**CRITICAL** It is important that all items are clean before using them for crystallization setups. All experimental steps, when sample is exposed to air, should be performed within a clean-air flow hood.

## PROCEDURE

### Membrane protein reconstitution in LCP. TIMING 15 min

**1)** Transfer 15 μL of molten 9.9 MAG into syringe #1, and 10 μL of protein solution into syringe #2. Connect syringes together using a syringe coupler, trying to minimize the amount of trapped air. Homogenize the sample by pushing it through the coupler back-and-forth between syringes, until a transparent LCP forms.

### Setting up crystallization in syringes. TIMING 25 min

**2)** Move the entire LCP sample into syringe #2. Disconnect empty syringe #1, while keeping the coupler connected to syringe #2.

**3)** Attach a removable needle to a 100 μL syringe (#3), and aspirate about 60 μL of the precipitant solution, selected by high-throughput crystallization screening and optimization.

<TROUBLESHOOTING>

**4)** Disconnect the needle from syringe #3, keeping the teflon ferrule inside the syringe.

**5)** Connect syringe #3 to the coupler attached to syringe #2. Carefully screw and tighten the coupler.

**6)** Inject about 5 μL protein laden LCP sample from syringe #2 into syringe #3. Control the transferred volume by the scale-reading on both syringes (both plungers should move by about 5 μL).

**CRITICAL STEP** It is important that LCP is extruded as a continuous extended string, fully immersed in the precipitant solution (Figure 4).

**7)** Disconnect syringe #3 from the coupler and attach a needle stopper to it.

**CRITICAL STEP** Watch for the LCP string when disconnecting the syringe from the coupler. Make sure that LCP does not adhere to the coupler needle during the coupler withdrawal.

**8)** Use Parafilm strips to seal the needle stopper and the plunger syringe interface (Figure 4).

**CRITICAL STEP** Incomplete sealing may lead to dehydration of the sample, which could affect phase properties of the lipidic mesophase and crystal formation.

**9)** Repeat Steps 3–8 to set up crystallization in 4 additional syringes (#4–7).

**10)** Place syringes #3–7 in a Ziploc bag, adding a moist fiber-free tissue to maintain a high level of humidity. Seal the Ziploc bag and store it in a 20 °C incubator.

**CRITICAL STEP** Storing syringes in a Ziploc bag with a moist tissue is essential to prevent dehydration and improve reproducibility.

### Incubation and inspection. TIMING 1–3 days

**11)** Inspect the samples directly inside syringes every 12 h, using a stereo zoom microscope equipped with cross-polarizers. Microcrystals typically appear within 1–3 d and can be detected as a faint uniform glow or as densely packed bright dots under cross-polarizers (Figure 4).

<TROUBLESHOOTING>

**PAUSE POINT**. Microcrystals grown in syringes can be stored for several days at 20 °C. Avoid large temperature fluctuations (over 2 °C) during sample storage and inspections. Samples in syringes can be transported at this stage to the XFEL source using a Greenbox thermal management system, pre-equilibrated at 20 °C.

### Sample consolidation and titration with 7.9 MAG. TIMING 15 min

**12)** Take out all the samples from the 20 °C incubator about 1 h before the expected start of LCP-SFX data collection.

**13)** Carefully remove Parafilm seals from syringe #3.

**14)** Replace the needle stopper with a removable needle.

**15)** Slowly push the plunger of syringe #3, squeezing out precipitant through the needle.

**CRITICAL STEP** Push the plunger of syringe #3 slowly and carefully. Harsh motion could accidentally squeeze out some LCP along with the precipitant solution, resulting in a sample loss.

**16)** Stop pushing the plunger when most of the precipitant solution is removed.

**17)** Replace the removable needle with a needle stopper.

**18)** Repeat Steps 13–17 with syringes #4–7.

**19)** Remove needle stoppers from syringes #3 and #4 and connect them together using a syringe coupler.

**20)** Transfer all sample from syringe #4 into syringe #3.

**21)** Repeat steps 19–20 with syringes #5–7 to consolidate the entire sample in syringe #3.

Squeeze out as much precipitant as possible.

**22)** Transfer about 5 μL of 7.9 MAG into a clean 100 μL syringe (#2), and connect syringes #3 and #2 through a coupler.

**23)** Homogenize the sample by moving it through the coupler back-and-forth between syringes.

**24)** Repeat steps 22–23 until the sample becomes fully homogeneous and transparent.

**CRITICAL STEP** Since the exact amount of residual precipitant solution is unknown, 7.9 MAG is titrated in 5 μL increments. For a 25 μL of original LCP sample, typically, about 10–15 μL of precipitant remains and about 15 μL of 7.9 MAG is needed to fully absorb the residual precipitant, making the final sample volume just over 50 μL.

<TROUBLESHOOTING>

**25)** Move the entire sample into syringe #2 and disconnect syringe #3.

### Microcrystal characterization. TIMING 15 min

**26)** Attach an LCP-injector loading needle (1 inch long, gauge 22, point style 3) to syringe #2.

**27)** Extrude ~1 μL of the sample onto a glass slide, cover with a glass cover slip and gently press on the cover to sandwich the sample.

**28)** Take images through a high magnification microscope with a brightfield illumination mode and under cross-polarizers. If possible, taking UV fluorescence and SONICC images can help to better characterize the sample (Figure 5).

**29)** Estimate crystal size and density (Figure 6). The minimum crystal size is about 1 μm. The minimum crystal density that will work depends on the crystal size, the size of the beam, the diameter of the injector's nozzle and the diffraction strength (see section "Crystal Density and Hit Rate" for guidelines). If the crystal density is too high (Figure 6a; too many multiple hits), then perform Steps 30–34. Otherwise proceed to step 35.

**CRITICAL STEP** This imaging step is critical to ensure that only the best samples are used for LCP-SFX data collection. Testing samples at the beamline without pre-screening them may waste ~60 min of valuable XFEL beamtime, if the crystals are too small or the crystal density is too low.

### Adjustment of crystal density. TIMING 10 min (OPTIONAL)

**30)** Prepare the volume of LCP as needed for dilution using 50 %v/v 7.9 MAG and 50 %v/v precipitant solution with two clean 100 μL syringes (washed and dried syringes #3 and #4) and a coupler, as described in Step 1.

**31)** Move the entire 7.9 MAG LCP sample into syringe #3. Disconnect syringe #4 keeping the coupler connected to syringe #3.

**32)** Connect syringe #2, containing the LCP with microcrystals, to the coupler attached to syringe #3.

**33)** Homogenize the contents of the two syringes by moving the sample back-and-forth between syringes about 100 times.

**34)** Repeat Steps 26–29 to re-evaluate the size and density of microcrystals.

### Load sample in LCP injector for LCP-SFX data collection. TIMING 5 min

**35)** Attach an LCP injector loading needle (1 inch long, gauge 22, point style 3) to syringe #2 that contains the final LCP sample homogeneously filled with microcrystals.

**36)** Transfer the sample into an LCP-injector.

**37)** Insert the LCP injector loaded with sample into the sample chamber, start the injector, adjust the LCP flow-rate based on the XFEL repetition pulse rate and the detector readout rate, and collect LCP-SFX data. The data collection details used to generate the results shown in this protocol are described in the Anticipated Results section and Refs. 13 and 17. The details of the data collection will depend on the specific beamline, the hardware and the software used.

**TIMING**.

**Membrane protein reconstitution in LCP**. TIMING 15 min

**Setting up crystallization in syringes**. TIMING 25 min

**Incubation and inspection**. TIMING 1–3 d

**Sample consolidation and titration with 7.9 MAG**. TIMING 15 min

**Microcrystal characterization**. TIMING 15 min

**Adjustment of crystal density**. TIMING 10 min (OPTIONAL)

**Loading sample in LCP injector for LCP-SFX data collection**. TIMING 5 min

**Box 1 Reconstitution of soluble protein crystals in LCP**. TIMING 30 min

**TROUBLESHOOTING**

| Step | Problem | Possible reasons | Solution |
|---|---|---|---|
| Reagent Setup | Lipid sample is not passing through the filter | Some MAGs are solid at room temperature, and they should be melted before the filtering step. However, they may still solidify during this centrifugation process and clog the filter tube. | Heat the lipid sample again or centrifuge at higher temperature (for example, at 40 °C). |
| 3 | Precipitant solution cannot be aspirated. | Clogged needle | Clean the needle with methanol or exchange to another needle. |
| | | Broken seal between the removable needle and the syringe. | Check that Teflon ferrule is present, and that the removable hub is properly attached and finger-tight. |
| | | Loose Teflon plunger tip. | The Teflon tip at the end of the plunger wears out after frequent use, and should be replaced when the seal is compromised. |

| Step | Problem | Possible reasons | Solution |
|---|---|---|---|
| 11 | No convincing crystals are observed under microscope. | The scaled-up conditions for crystal nucleation are slightly different from those found during the high-throughput screening. | Set up a small gradient screen in syringes around the original condition. |
| | | Crystals are too small to be detected. | Detection of small microcrystals inside a syringe could be difficult. To have a better view of the sample, extrude about 1 μL of the LCP sample from the syringe and examine it as described in the Microcrystal Characterization section, Steps 26–29. |
| 24 | Phase changes upon titration with 7.9 MAG. | Too much titration lipid is added. | Overloading the titration lipid will lead to a lower hydration of the sample and may induce a phase change. By adding back few microliters of precipitant, the hydration should be restored. |

## ANTICIPATED RESULTS

Two examples of GPCR structures determined by LCP-SFX approach are presented below.

### Human serotonin receptor 2B (5-$HT_{2B}$) in complex with ergotamine

Human serotonin receptor 2B (5-$HT_{2B}$) is a member of the class A G protein-coupled receptor (GPCR) superfamily. It responds to a neurotransmitter serotonin, mediating a variety of biological functions in the central and peripheral neural systems. To improve the receptor's stability and aid in its crystallization, the human wild type 5-$HT_{2B}$ sequence was modified by replacing residues Tyr249-Val313 from the intracellular loop 3 (ICL3) with a thermostabilized apocytochrome $b_{562}$ RIL (BRIL), truncating 35 N-terminal and 76 C-terminal residues, and introducing a thermostabilizing mutation M144W[43]. The resultant engineered construct was expressed in baculovirus infected *Sf*9 insect cells, solubilized in a dodecyl maltoside (DDM) / cholesteryl hemisuccinate (CHS) detergent mixture in the presence of an anti-migraine drug ergotamine, and purified by a metal affinity chromatography[43].

The purified 5-$HT_{2B}$/ergotamine complex at a concentration of 20 mg/mL was reconstituted in LCP composed of 10 %w/w cholesterol / 90 %w/w monoolein. Initial high-throughput LCP crystallization trials were performed in 96-well glass sandwich plates (Marienfeld)[22] using an NT8-LCP crystallization robot (Formulatrix) and home-made PEG400/salt crystallization screens[44]. Protein-laden LCP was dispensed in 40 nL droplets and overlaid with 800 nL of precipitant solution. Plates were incubated and imaged at 20 °C using an automatic incubator/imager RockImager 1000 (Formulatrix). Initial crystal hits were observed in several conditions. Conditions with magnesium sulphate were optimized further to obtain relatively large crystals (80 μm × 20 μm × 10 μm) for traditional microcrystallography at a synchrotron source (Figure 7a,b)[43], while conditions with magnesium chloride, which reproducibly yielded high density microcrystals, were used to prepare samples for LCP-SFX (Figure 7c,d)[17].

Crystals optimized for traditional crystallography were harvested directly from LCP using MiTeGen micromounts and flash frozen in liquid nitrogen. Crystallographic data were

collected at the 23ID-D beamline of the Advanced Photon Source (APS), Argonne, IL using 10 μm minibeam at a wavelength of 1.0330 Å and a MarMosaic 300 CCD detector. Data from the 17 best crystals collected under cryo-conditions were merged together and used to solve the structure by molecular replacement at 2.7 Å resolution[43].

Samples for LCP-SFX were prepared in syringes as outlined in the protocols above using 90 %w/w monoolein/ 10 %w/w cholesterol as the LCP host lipid and 100 mM Tris/HCl pH 8.0, 20–80 mM $MgCl_2$, 30%(v/v) PEG 400 as precipitant conditions. Seven samples with a total volume of 100 μL were prepared at magnesium chloride concentrations ranging between 20 and 80 mM. Crystallization in syringes was set up in the home laboratory 2 days before the experiment start date. After an overnight incubation at 20 °C, all samples were transported to LCLS in a Greenbox (Thermosafe Brands) pre-equilibrated at 20 °C. Before loading the samples into the LCP injector, they were titrated with 7.9 MAG and imaged under visual, UV-fluorescence and SONICC microscopes to estimate crystals size (~5 μm) and density (Figure 7c,d)[17].

LCP-SFX data were collected at the CXI endstation of LCLS, Stanford, CA, using 50 fs X-ray pulses ($3{\cdot}10^{10}$ photons/pulse) at a repetition rate of 120 Hz and a wavelength of 1.3 Å, focused to a 1.5 μm spot size by Kirkpatrick-Baez mirrors. LCP with randomly dispersed 5-$HT_{2B}$/ergotamine microcrystals was extruded through a 20–50 μm in diameter nozzle into a vacuum chamber at room temperature and at a constant flow rate of 50–200 nL/min, which was intersected with the XFEL beam. Singe shot diffraction images (Figure 7e) were collected by a Cornell-SLAC Pixel Array Detector (CSPAD) located at a distance of 100 mm from the sample. A total of 4,217,508 diffraction patterns were collected within 10 h using about 0.3 mg of protein. Of these patterns, 152,651 were identified as crystal hits, corresponding to a hit rate of 3.6 %. Of these crystal hits, 32,819 patterns (21.5 %) were successfully indexed and integrated by CrystFEL[4]. The structure was determined by molecular replacement at 2.8 Å resolution (Figure 7f).

### Human smoothened receptor in complex with cyclopamine

Smoothened receptor (SMO) belongs to the class Frizzled GPCRs. It participates in the hedgehog signalling pathway and is involved in embryonic development and tumour growth. The native agonist for SMO is not known, however a number of small molecule agonists and antagonists, including a naturally occurring teratogen cyclopamine[45] have been recently identified.

For structural studies, the wild type human SMO was modified by truncating the N-terminal cysteine-rich domain (residues 1–181) and C-terminal residues (at Q555), and fusing BRIL in place of ICL3 residues 434–440[13]. The engineered construct was expressed in baculovirus infected *Sf*9 insect cells, solubilized in DDM/CHS in the presence of cyclopamine, purified by metal affinity chromatography and concentrated to 50 mg/mL.

Initial high-throughput LCP crystallization trials for SMO/cyclopamine were performed as described above for 5-$HT_{2B}$/ergotamine. After extensive optimization, relatively large crystals (120 μm × 10 μm × 5 μm) obtained in conditions with ammonium salts were used for data collection at a synchrotron source (Figure 8a,b), while microcrystals obtained in 100

mM Hepes pH 7.0, 30 % (v/v) PEG 400, 100 mM NaCl were used for LCP-SFX data collection (Figure 8c,d). Data collected at APS on the large cryo-cooled SMO/cyclopamine crystals suffered from poor diffraction and high mosaicity, and thus did not yield a structure.

Following the protocols described in this article, we prepared 80 μL of LCP filled with SMO/cyclopamine microcrystals (Figure 8c,d). LCP–SFX data were collected at LCLS using the same parameters as those described for 5-$HT_{2B}$/ergotamine samples above (Figure 8e). A total of 3,510,525 diffraction patterns were collected, of which 274,214 were identified as potential single crystal diffraction patterns, corresponding to an average hit rate of 7.8 %. Autoindexing and structure factor integration of the crystal hits was performed using CrystFEL[4] resulting in 61,964 indexed images (22.6% indexing success rate). Because of a strong anisotropy, the LCP-SFX data were analysed by the UCLA anisotropy server (http://www.services.mbi.ucla.edu/anisoscale/) and truncated at 3.4, 3.2 and 4.0 Å resolution along the three principal axes[13]. The structure was solved by molecular replacement and revealed the location of cyclopamine in a narrow and long cavity spanning from the extracellular loop into the transmembrane helical barrel (Figure 8f).

## Acknowledgments

This work was supported by the National Institutes of Health grants P50 GM073197 and U54 GM094618. We thank K. Kadyshevskaya for assistance with figure preparation, L. Johansson for comments, and A. Walker for assistance with manuscript preparation.

## REFERENCES

1. Neutze R, Wouts R, van der Spoel D, Weckert E, Hajdu J. Potential for biomolecular imaging with femtosecond X-ray pulses. Nature. 2000; 406:752–757. [PubMed: 10963603]
2. Chapman HN, et al. Femtosecond X-ray protein nanocrystallography. Nature. 2011; 470:73–77. [PubMed: 21293373]
3. Spence JC, Weierstall U, Chapman HN. X-ray lasers for structural and dynamic biology. Rep. Prog. Phys. 2012; 75:102601. [PubMed: 22975810]
4. White TA, et al. Crystallographic data processing for free-electron laser sources. Acta Crystallogr. D Biol. Crystallogr. 2013; 69:1231–1240. [PubMed: 23793149]
5. DePonte DP, et al. Gas Dynamic Virtual Nozzle for Generation of Microscopic Droplet Streams. J. Phys. D. 2008; 41:195505.
6. Lomb L, et al. An anti-settling sample delivery instrument for serial femtosecond crystallography. J. Appl. Cryst. 2012; 45:674–678. doi:
7. Johansson LC, et al. Lipidic phase membrane protein serial femtosecond crystallography. Nat. Methods. 2012; 9:263–265. [PubMed: 22286383]
8. Boutet S, et al. High-resolution protein structure determination by serial femtosecond crystallography. Science. 2012; 337:362–364. [PubMed: 22653729]
9. Redecke L, et al. Natively inhibited Trypanosoma brucei cathepsin B structure determined by using an X-ray laser. Science. 2013; 339:227–230. [PubMed: 23196907]
10. Johansson LC, et al. Structure of a photosynthetic reaction centre determined by serial femtosecond crystallography. Nat. Commun. 2013; 4:2911. [PubMed: 24352554]
11. Kern J, et al. Room temperature femtosecond X-ray diffraction of photosystem II microcrystals. Proc. Natl. Acad. Sci. USA. 2012; 109:9721–9726. [PubMed: 22665786]
12. Sierra RG, et al. Nanoflow electrospinning serial femtosecond crystallography. Acta Crystallogr. D Biol. Crystallogr. 2012; 68:1584–1587. [PubMed: 23090408]
13. Weierstall U, et al. Lipidic cubic phase injector facilitates membrane protein serial femtosecond crystallography. Nat. Commun. 2014; 5:3309. [PubMed: 24525480]

14. Larsson K. Cubic lipid-water phases: structures and biomembrane aspects. J. Phys. Chem. 1989; 93:7304–7314.
15. Cherezov V. Lipidic cubic phase technologies for membrane protein structural studies. Curr. Opin. Struct. Biol. 2011; 21:559–566. [PubMed: 21775127]
16. Landau EM, Rosenbusch JP. Lipidic cubic phases: a novel concept for the crystallization of membrane proteins. Proc. Natl. Acad. Sci. USA. 1996; 93:14532–14535. [PubMed: 8962086]
17. Liu W, et al. Serial femtosecond crystallography of G protein-coupled receptors. Science. 2013; 342:1521–1524. [PubMed: 24357322]
18. Zarrine-Afsar A, et al. Crystallography on a chip. Acta Crystallogr. D Biol. Crystallogr. 2012; 68:321–323. [PubMed: 22349234]
19. Frank M, et al. Femtosecond X-ray diffraction from two-dimensional protein crystals. IUCrJ. 2014; 1:95–100. doi:
20. Gati C, et al. Serial crystallography on in vivo grown microcrystals using synchrotron radiation. IUCrJ. 2014; 1:87–94. doi:
21. Kimura T, et al. Imaging live cell in micro-liquid enclosure by X-ray laser diffraction. Nat. Commun. 2014; 5:3052. [PubMed: 24394916]
22. Cherezov V, Peddi A, Muthusubramaniam L, Zheng YF, Caffrey M. A robotic system for crystallizing membrane and soluble proteins in lipidic mesophases. Acta Crystallogr. D Biol. Crystallogr. 2004; 60:1795–1807. [PubMed: 15388926]
23. Caffrey M, Cherezov V. Crystallizing membrane proteins using lipidic mesophases. Nat. Protoc. 2009; 4:706–731. [PubMed: 19390528]
24. Liu W, Cherezov V. Crystallization of membrane proteins in lipidic mesophases. J. Vis. Exp. 2011; 49:e2501.
25. Li D, Boland C, Walsh K, Caffrey M. Use of a robot for high-throughput crystallization of membrane proteins in lipidic mesophases. J. Vis. Exp. 2012; 67:e4000. [PubMed: 22971907]
26. Kulkarni CV, Wachter W, Iglesias-Salto G, Engelskirchen S, Ahualli S. Monoolein: a magic lipid? Phys. Chem. Chem. Phys. 2011; 13:3004–3021. [PubMed: 21183976]
27. Li D, Shah ST, Caffrey M. Host Lipid and Temperature as Important Screening Variables for Crystallizing Integral Membrane Proteins in Lipidic Mesophases. Trials with Diacylglycerol Kinase. Cryst. Growth Des. 2013; 13:2846–2857.
28. Li D, et al. Crystallizing Membrane Proteins in the Lipidic Mesophase. Experience with Human Prostaglandin E2 Synthase 1 and an Evolving Strategy. Cryst. Growth Des. 2014; 14:2034–2047.
29. Cherezov V, Clogston J, Misquitta Y, Abdel-Gawad W, Caffrey M. Membrane protein crystallization in meso: lipid type-tailoring of the cubic phase. Biophys. J. 2002; 83:3393–3407. [PubMed: 12496106]
30. Cherezov V, et al. High-resolution crystal structure of an engineered human beta2-adrenergic G protein-coupled receptor. Science. 2007; 318:1258–1265. [PubMed: 17962520]
31. Qiu H, Caffrey M. Lyotropic and Thermotropic Phase Behavior of Hydrated Monoacylglycerols: Structure Characterization of Monovaccenin. J. Phys. Chem. B. 1998; 102:4819–4829.
32. Qiu H, Caffrey M. The phase diagram of the monoolein/water system: metastability and equilibrium aspects. Biomaterials. 2000; 21:223–234. [PubMed: 10646938]
33. Misquitta LV, et al. Membrane protein crystallization in lipidic mesophases with tailored bilayers. Structure. 2004; 12:2113–2124. [PubMed: 15576026]
34. Misquitta Y, et al. Rational design of lipid for membrane protein crystallization. J. Struct. Biol. 2004; 148:169–175. [PubMed: 15477097]
35. Cherezov V, Fersi H, Caffrey M. Crystallization screens: compatibility with the lipidic cubic phase for in meso crystallization of membrane proteins. Biophys. J. 2001; 81:225–242. [PubMed: 11423409]
36. Joseph JS, et al. Characterization of lipid matrices for membrane protein crystallization by high-throughput small angle X-ray scattering. Methods. 2011; 55:342–349. [PubMed: 21903166]
37. van't Hag L, et al. In Meso Crystallization: Compatibility of Different Lipid Bicontinuous Cubic Mesophases with the Cubic Crystallization Screen in Aqueous Solution. Cryst. Growth Des. 2014; 14:1771–1781.

38. Landau EM, Rummel G, Cowan-Jacob SW, Rosenbusch JP. Crystallization of a Polar Protein and Small Molecules from the Aqueous Compartment of Lipidic Cubic Phases. J. Phys. Chem. B. 1997; 101:1935–1937.

39. Caffrey M. A lipid's eye view of membrane protein crystallization in mesophases. Curr. Opin. Struct. Biol. 2000; 10:486–497. [PubMed: 10981640]

40. Cherezov V, Clogston J, Papiz MZ, Caffrey M. Room to move: crystallizing membrane proteins in swollen lipidic mesophases. J. Mol. Biol. 2006; 357:1605–1618. [PubMed: 16490208]

41. Wadsten P, et al. Lipidic sponge phase crystallization of membrane proteins. J. Mol. Biol. 2006; 364:44–53. [PubMed: 17005199]

42. Owen RL, et al. Outrunning free radicals in room-temperature macromolecular crystallography. Acta Crystallogr. D Biol. Crystallogr. 2012; 68:810–818. [PubMed: 22751666]

43. Wacker D, et al. Structural features for functional selectivity at serotonin receptors. Science. 2013; 340:615–619. [PubMed: 23519215]

44. Xu F, Liu W, Hanson MA, Stevens RC, Cherezov V. Development of an Automated High Throughput LCP-FRAP Assay to Guide Membrane Protein Crystallization in Lipid Mesophases. Cryst. Growth Des. 2011; 11:1193–1201.

45. Taipale J, et al. Effects of oncogenic mutations in Smoothened and Patched can be reversed by cyclopamine. Nature. 2000; 406:1005–1009. [PubMed: 10984056]

46. Liu, W. PhD thesis. The Ohio State University; 2007. Membrane protein crystallization in the lipidic cubic phase: testing hypotheses relating to reconstitution.

**Box 1 Reconstitution of soluble protein crystals in LCP. TIMING 30 min**

1. Prepare a suspension of soluble protein microcrystals in a precipitant solution. Estimate crystal size and density (steps 26–29 of the main protocol). Adjust the crystal density if needed.
2. Test compatibility of the precipitant solution, which was used to crystallize the protein, with LCP using 7.9 MAG, 9.7 MAG or 1:1 mixture of 7.9 MAG/9.9 MAG as the host lipid.
3. Transfer 25 μL of microcrystal suspension into syringe #1, and 25 μL of the best LCP host lipid, identified in step 2, into syringe #2.
4. Connect syringes #1 and #2 through a coupler.
5. Homogenize the contents of the syringes by moving the sample back-and-forth between syringes until a homogeneous and transparent LCP forms.
6. Evaluate the crystal size and the density of crystals in the final sample (steps 26–29 of the main protocol).

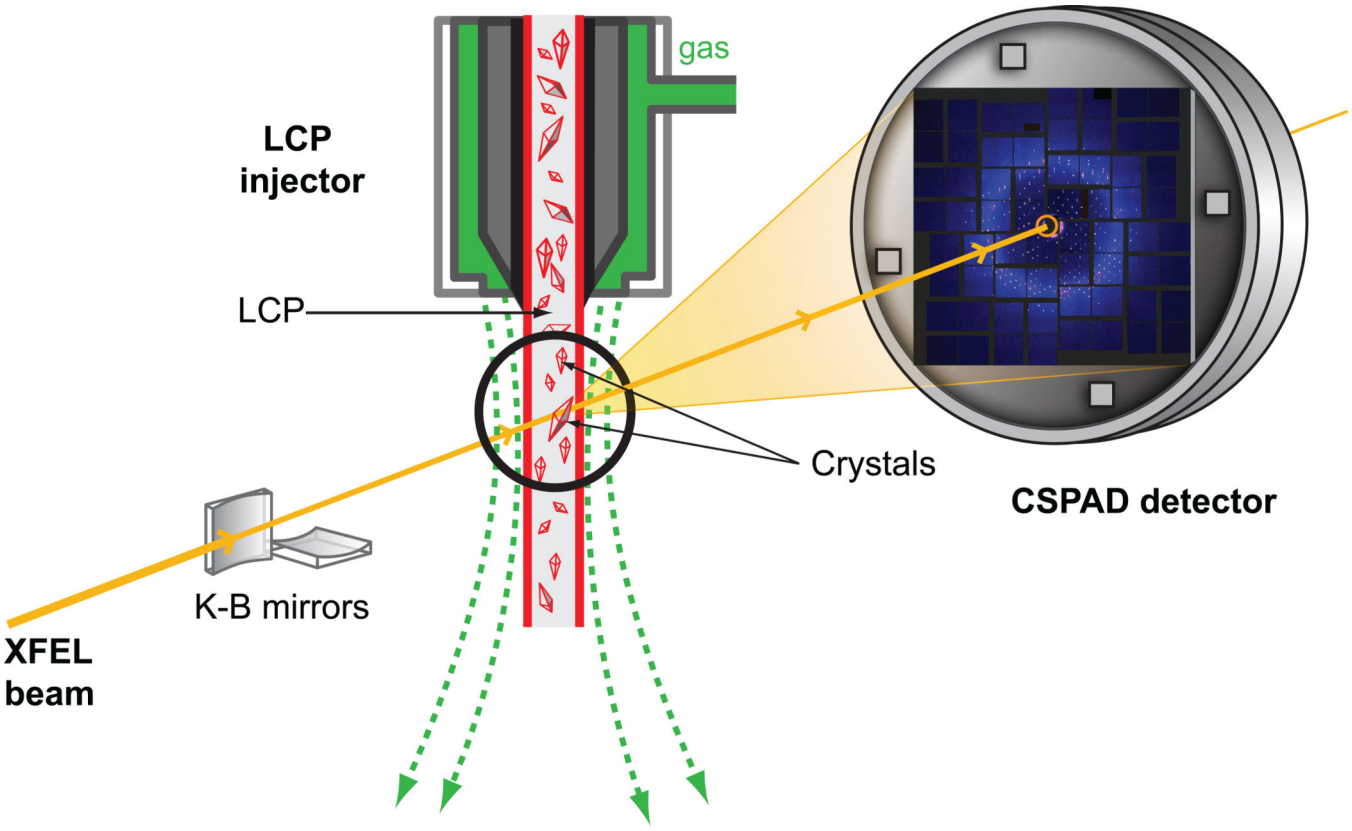


**Figure 1. Schematic diagram of an LCP-SFX experiment at LCLS**

LCP jet delivers crystals in a continuous stream of LCP to the interaction point with an incident XFEL beam focused to a 1.5 μm diameter spot by Kirkpatrick-Baez (K-B). Single shot diffraction patterns from microcrystals at different orientations are recorded by a Cornell-SLAC Pixel Array Detector (CSPAD) at 120 Hz. LCP jet, the detector and the entire XFEL beam path are under vacuum.

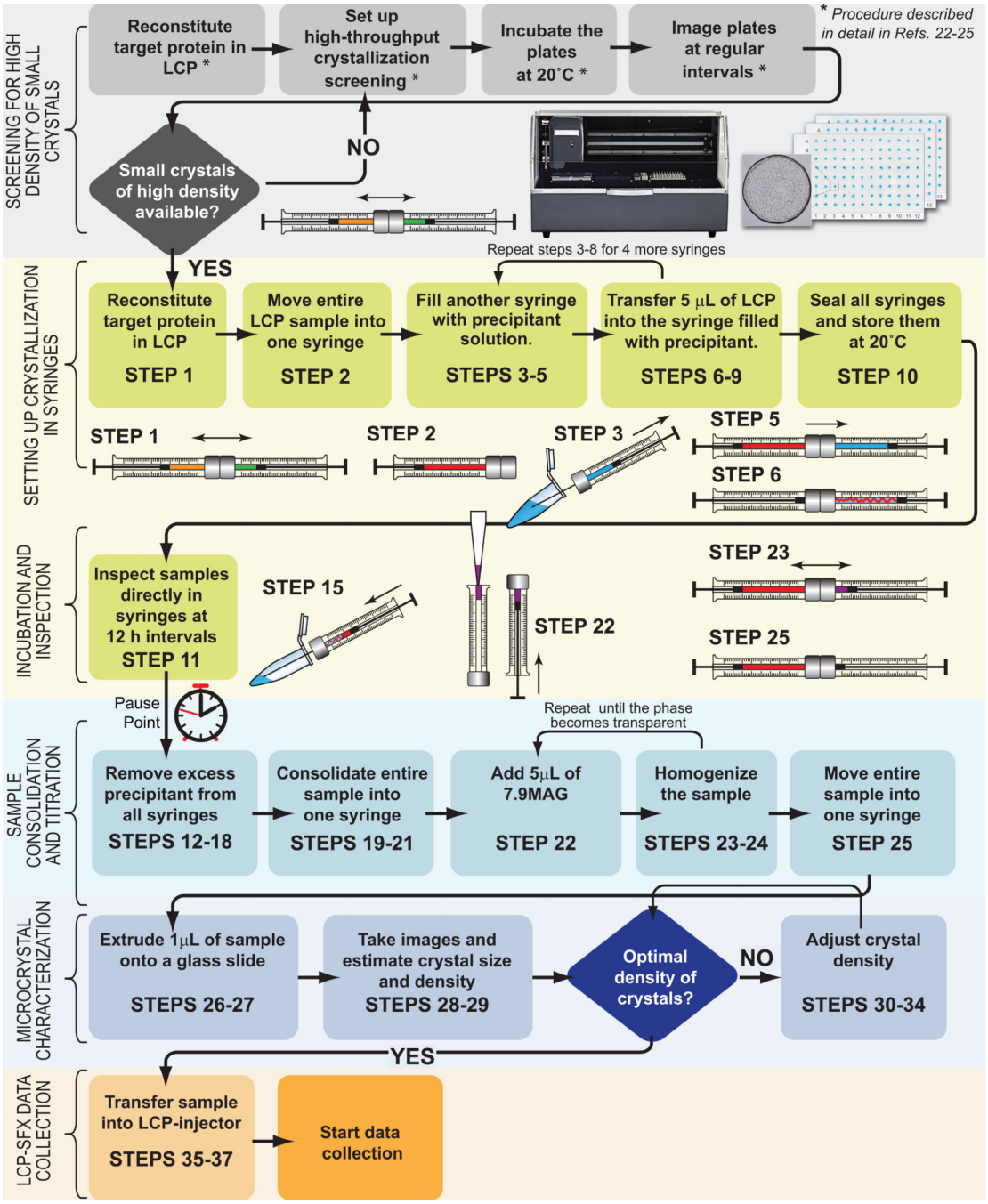


**Figure 2. Flowchart of sample preparation for LCP-SFX**

Each stage of the sample preparation procedure is divided into several steps. The schematic images of the syringes illustrate critical steps of sample preparation. Different substances are labeled with different colors (LCP host lipid – orange, protein solution – green, LCP – red, precipitant solution – blue, 7.9 MAG – purple).

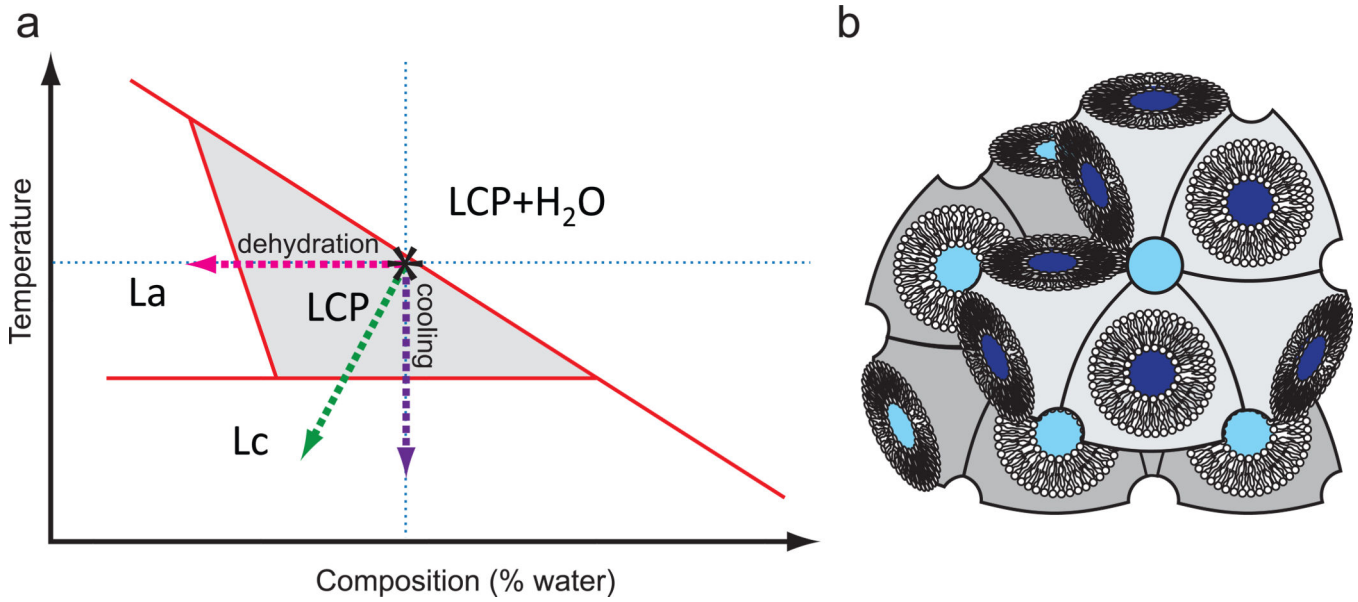


**Figure 3. Phase behavior of MAG lipids**

(**a**) Simplified temperature-composition phase diagram for monoacylglycerol lipids (MAGs). The exact phase transition boundaries depend on the lipid nature, detergent concentration and composition of the precipitant. The area that corresponds to pure LCP is shaded. Crystallization experiments are performed at room temperature and at the full hydration boundary (marked by an asterisk). Evaporative dehydration upon injection of LCP in vacuum is shown by a green dashed line. (**b**) Cartoon representation of a lipidic cubic phase.

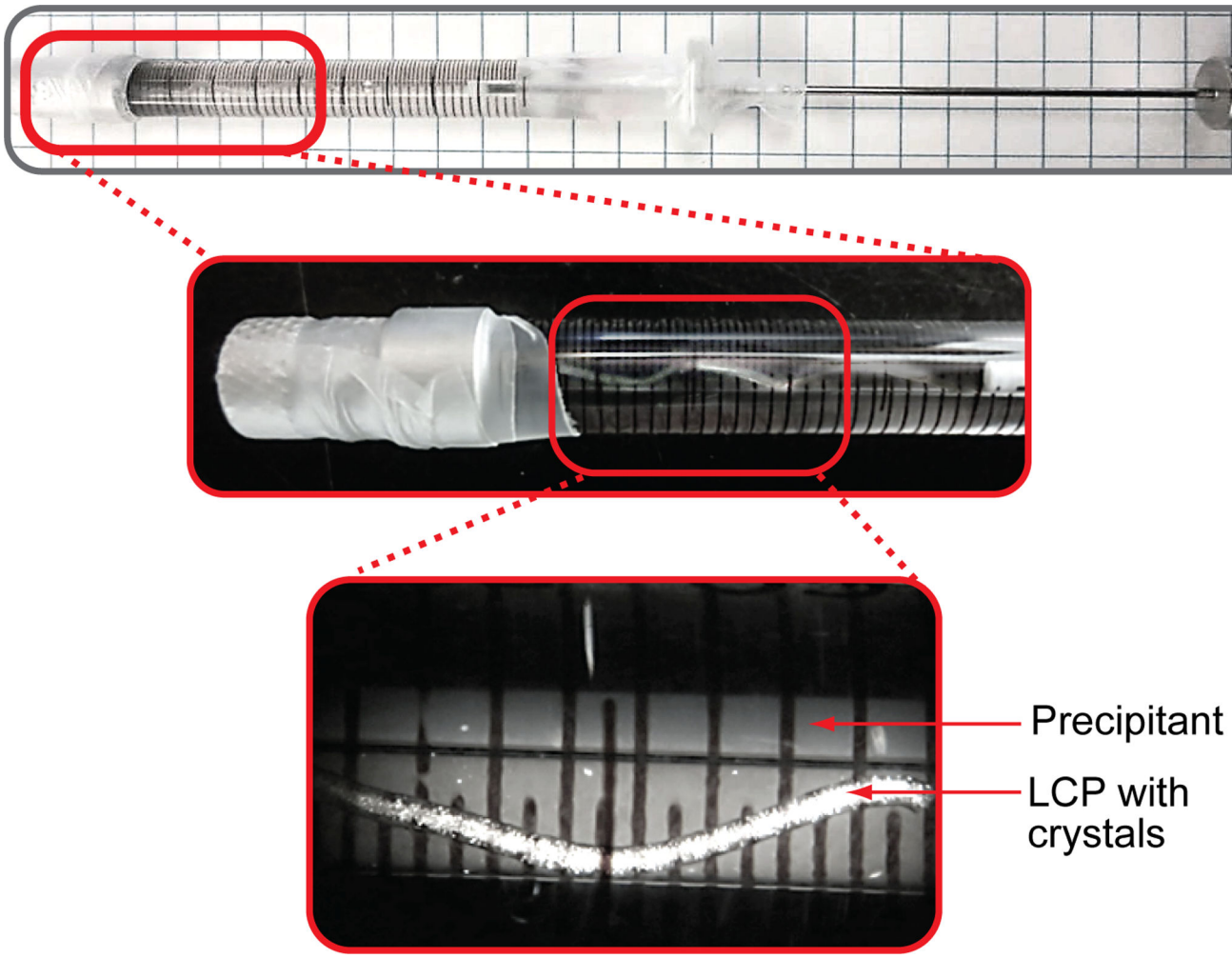


**Figure 4. Crystallization setup in syringes**

Photographs of a syringe containing 60 μL of precipitant and 5 μL of protein-laden LCP with microcrystals growing in it, at two zoom levels. The highest zoom photograph is taken under a stereo microscope equipped with cross-polarizers. Microcrystals are visible as bright dense dots inside of a snake-like LCP string. Other sparse bright objects are located outside of the syringe barrel.

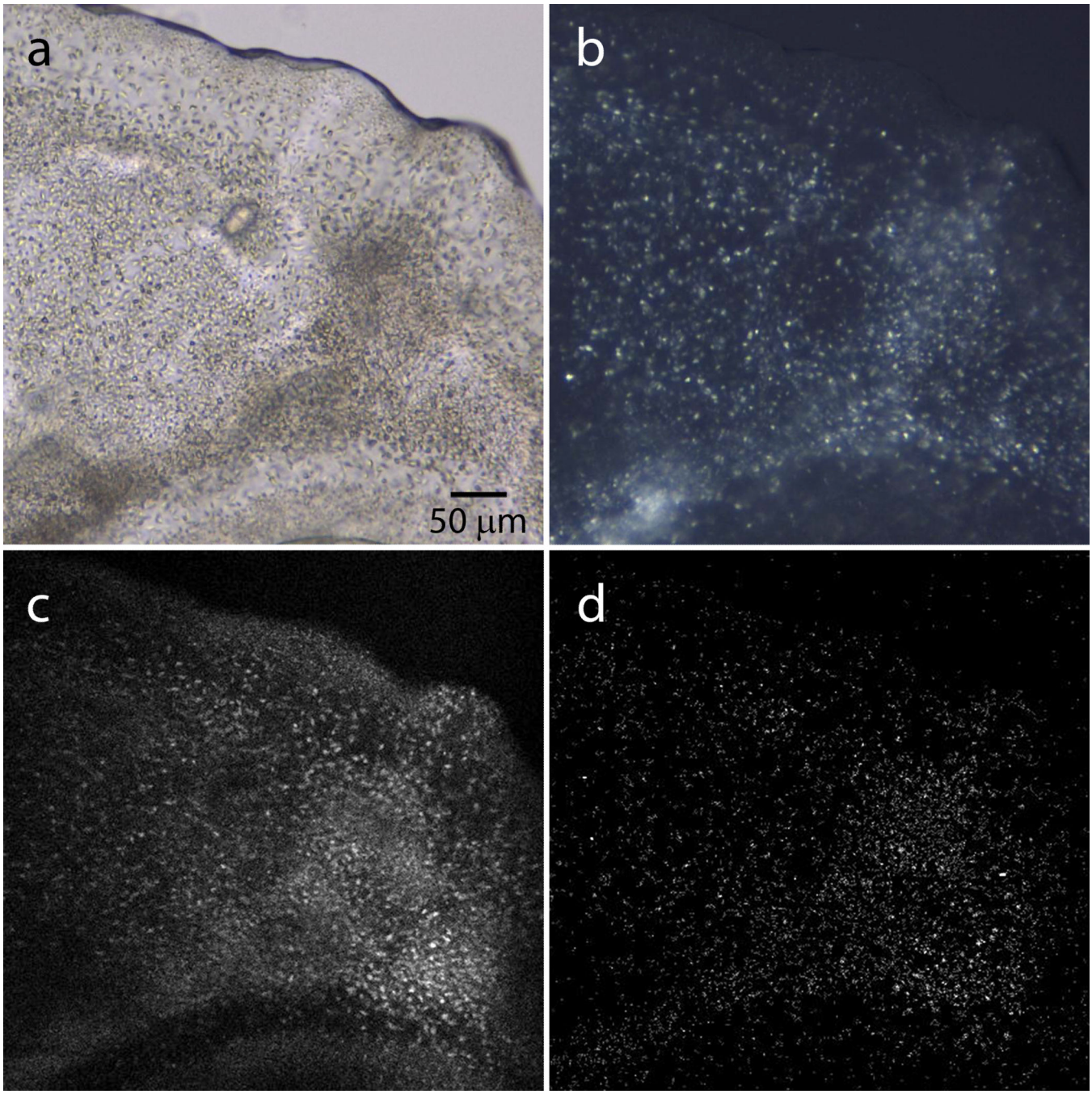


**Figure 5.**

Microcrystals of serotonin 5-$HT_{2B}$ receptor in LCP captured with different imaging profiles. (**a**) Bright-field imaging. (**b**) Cross polarized imaging. (**c**) UV two-photon fluorescence (UV-TPEF). (**d**) second harmonic generation (SHG) imaging. UV-TPEF and SHG images are taken by a SONICC imager (Formulatrix).

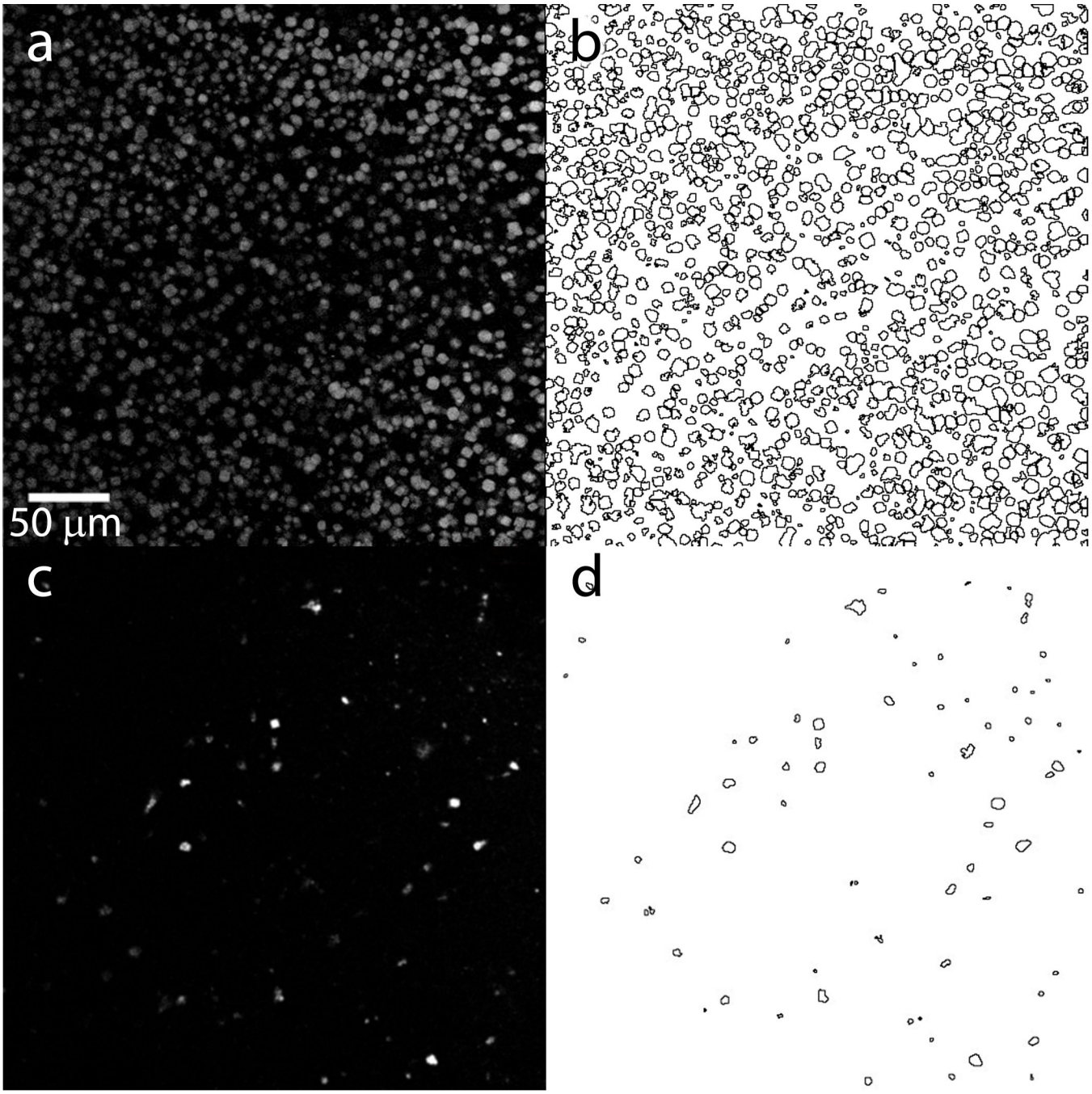


**Figure 6. Crystal density estimation**

(**a**) and (**c**) Single slice UV-TPEF images (depth of field ~20 μm) of two preparations of lysozyme crystals embedded in LCP captured by SONICC imager (Formulatrix). (**b**) and (**d**) Automatic crystal detection and counting is performed by the ImageJ program (http://imagej.nih.gov/ij/). The estimated total volume of the imaged slice within the depth of focus is $2.6 \cdot 10^{-3}$ μL. For (a) and (b) the total number of crystals is 1335, the average crystal size is 5.8 μm and the crystal density is $5 \cdot 10^{5}$ crystals $\mu L^{-1}$. Such crystal size and density is too high and will result in multiple hits with any LCP injector nozzle with diameter from 15 to

50 μm. For an optimal hit rate (~30–40 %) with 30 μm diameter LCP injector nozzle, the crystals should be diluted approximately 5 times. For (c) and (d) the total number of crystals is 71, the average crystal size is 4 μm and the crystal density is $2.7 \cdot 10^4$ crystals·$\mu L^{-1}$. This crystal size and density is quite low and will result in approximately 4 % hit rate with 30 μm diameter LCP injector nozzle.

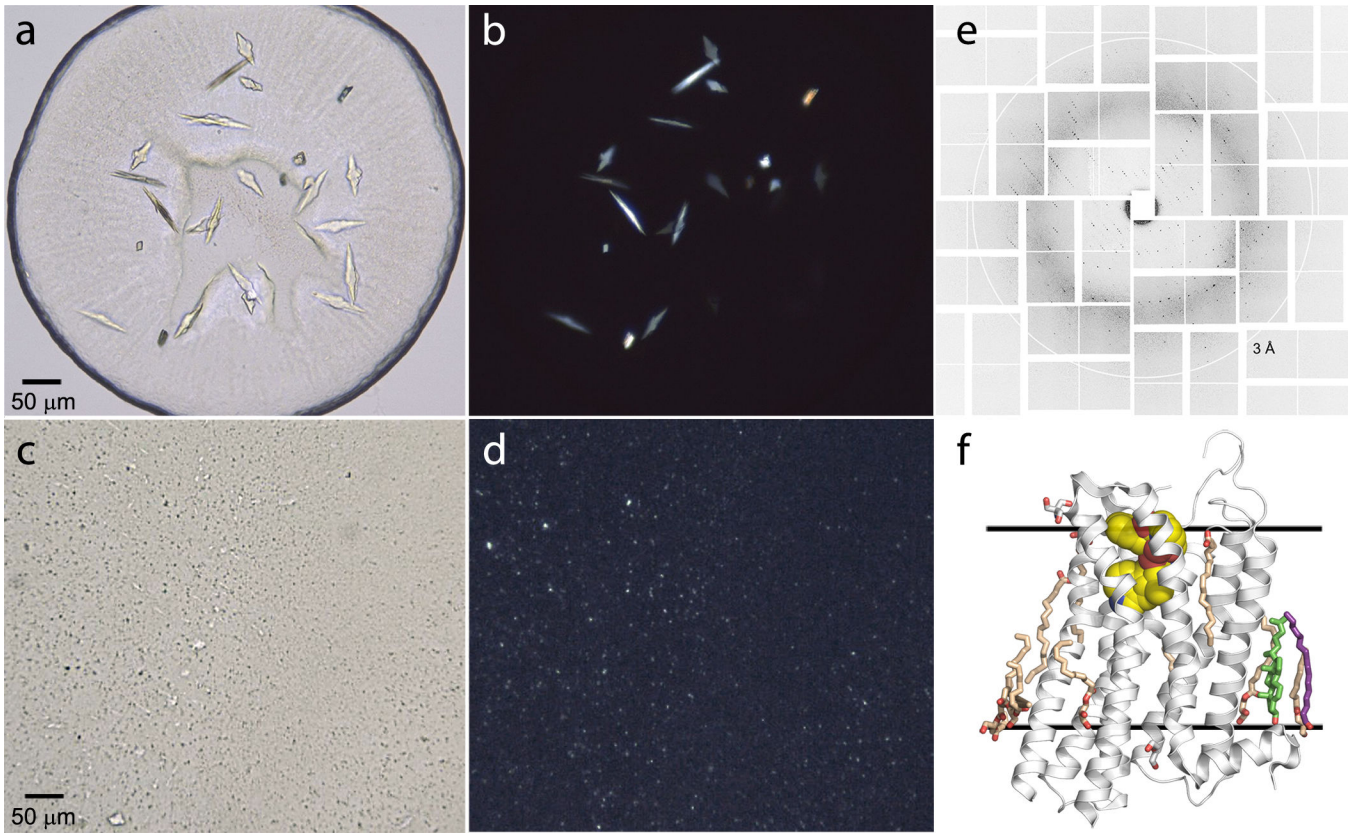


**Figure 7. Representative results, obtained with 5-HT$_{2B}$/ergotamine**

(**a**) Brightfield and (**b**) cross-polarized images of crystals used for synchrotron data collection. (**c**) Brightfield and (**d**) cross-polarized images of crystals used for LCP-SFX data collection. (**e**) Single shot XFEL diffraction image collected from a 5-HT$_{2B}$/ ergotamine microcrystal in LCP. (**f**) Cartoon representation of the 5-HT$_{2B}$/ergotamine structure obtained by LCP-SFX approach. Solid lines indicate approximate membrane boundaries.

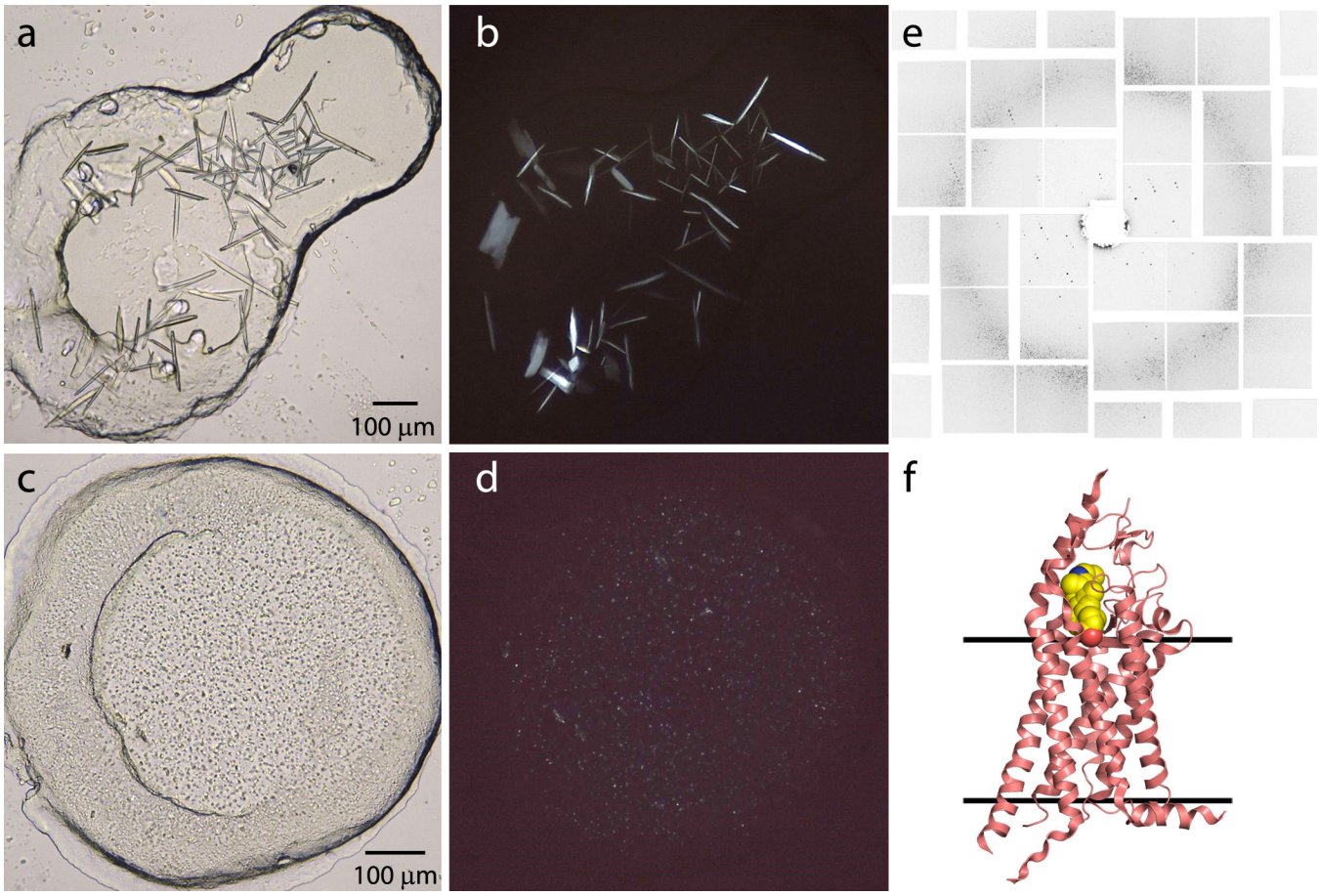


**Figure 8. Representative results, obtained with SMO/cyclopamine**

(**a**) Brightfield and (**b**) cross-polarized images of SMO/cyclopamine crystals (~120×10×5 μm) optimized for a synchrotron source. These large crystals had high mosaicity and poor diffraction. (**c**) Brightfield and (**d**) cross-polarized images of SMO/cyclopamine microcrystals (< 5 μm) used for LCP-SFX data collection. (**e**) Single shot XFEL diffraction image collected from a SMO/cyclopaminemicrocrystal in LCP. (**f**) Cartoon representation of the SMO/cyclopamine structure obtained by LCP-SFX approach. Solid lines indicate approximate membrane boundaries.

**Table 1**

LCP host lipids suitable for LCP-SFX

| Abbreviation[#] | Common Name | MW (Da) | LCP T range (°C) | Full hydration (%w/w)[*] | Lipid bilayer thickness (Å) [*] | Water channel diameter (Å) [*] | Number of unique proteins crystallized | Suppliers |
|---|---|---|---|---|---|---|---|---|
| 9.9 MAG | monoolein | 356.5 | 18 – 90[32] | ~40 | 35.6[46] | 46.4[46] | 49 | Nu Chek Prep, Sigma |
| 9.7 MAG | monopalmitolein | 328.5 | N/A | ~50 | 33.2[46] | 56.6[46] | 1 | Avanti Polar Lipids, Nu Chek Prep, Sigma |
| 11.7 MAG | monovaccenin | 356.5 | 20 – 85[31] | ~50 | N/A | N/A | 3 | Nu Chek Prep |
| 7.8 MAG | | 314.5 | N/A | ~50 | N/A | N/A | 2 | Avanti Polar Lipids |
| 7.9 MAG | | 328.5 | 6 – 85[34] | ~50 | N/A | N/A | 1 | Avanti Polar Lipids |
| 8.6 MAG | | 300.4 | N/A | N/A | N/A | N/A | 0 | Avanti Polar Lipids |
| 8.7 MAG | | 314.5 | N/A | ~50 | N/A | N/A | 0 | Avanti Polar Lipids |
| 8.8 MAG | | 328.5 | N/A | ~50 | N/A | N/A | 2 | Avanti Polar Lipids |
| 8.9 MAG | | 342.5 | N/A | N/A | N/A | N/A | 0 | Avanti Polar Lipids |

[*] Refers to the values at 20 °C or RT.

[#] In the N.T MAG notation, N corresponds to the number of carbon atoms in the acyl chain extending from the carboxyl carbon to the first carbon of the double bond, and T corresponds to the number of carbon atoms from the second carbon of the double bond to the methyl terminus.